Journal of Applied Electrochemistry **32**: 275–279, 2002.

A novel silver oxide electrode and its charge–discharge performance

H.T. LIU[1], X. XIA[1]* and Z.P. GUO[2]
[1]*Department of Chemistry, Xinjiang University, Urumqi, 830046, P.R. China*
[2]*Institute for Superconducting & Electronic Materials, University of Wollongong, NSW 2522, Australia*
*(*author for correspondence, e-mail: xxia@xju.edu.cn)*

Received 16 June 2001; accepted in revised form 15 January 2002

Key words: active material, discharge capacity, mass and charge transfer, mixed electrode, periodic charge–discharge

Abstract

Improvement of the conventional silver oxide electrode has been achieved by mixing with a certain amount of nanophase Ag_2O particles. The periodic charge–discharge results of various electrode compositions under different discharge conditions (e.g., 1*C*, *C*/3 and *C*/10) provides a clear comparison of electrochemical performance. When the nanophase Ag_2O species are between 10% and 35% of the active total amount, an extra 20–30% discharge capacity can be expected. However, if the electrode consists only of nanophase Ag_2O as active material, it does not have effective charge–discharge cycles. The favourable role of nanophase Ag_2O in a silver oxide electrode is attributed to the increased active material utilization because of optimum mass and charge transfer.

1. Introduction

Investigation of the behaviour of the silver oxide electrode in KOH solution has been extensively made because silver oxides form the positive active material of alkaline Ag–Zn and Ag–Cd storage batteries [1–6]. There is general agreement that silver oxide material consists of three types: Ag_2O, AgO and Ag_2O_3 [7]. Ag_2O with very high resistivity ($\sim 10^8$ Ω cm) as an intermediate product between charged final product AgO and discharged final Ag, itself has a great influence on charge–discharge performance of the secondary practical battery. To date, two basically different mechanisms have been found to be involved in Ag_2O film formation: one is a dissolution–precipitation process and the other a direct interfacial reaction [8–10]. On charge–discharge plots, there commonly appear two potential plateaux in the anodic and cathodic polarizing directions, and the relative length of the two plateaux is related to the rate of charge or discharge. The distribution of Ag_2O particles at the surface of an electrode influences the contour of the charge–discharge curves and could be beneficial to the charge–discharge performance of the silver oxide electrode by improving the utilization of Ag_2O active material during the process of cycling.

In recent years, nanophase techniques have been gradually applied in the field of material science and some achievements have been made. The application of nanophase material in the area of electrochemical power sources has been reported [11, 12]. However, the preparation of nanophase Ag_2O particles and their use as an active electrode material, have not yet been attempted. We have successfully synthesized various nanophase Ag_2O particles by different chemical methods, and the physical characteristics and the chemical formation mechanisms have been reported [13]. The nanophase Ag_2O particles (mean diameter 35 nm) used here were prepared by the principal reaction of $AgNO_3$ (AR grade, Beijing) with a certain amount of polyvinyl pyrrolidone (PVP) as a chelating agent for the Ag atom in a low concentration KOH (AR grade, Shanghai) solution.

The carbonyl oxygen atom of PVP, having lone-pair electrons, easily forms coordination species with the central Ag^+ ion which has several empty electron hybrid orbits. The formation of a covalent coordination bond enforces the electropositivity of the central ion, which makes it more convenient for the OH^- ion because of a smaller radius to approach Ag^+ and interact with it (Scheme 1).

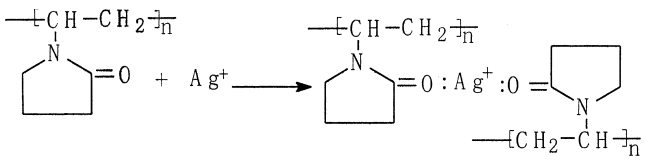

Due to the coordination effect taken by macromolecule PVP, the ions or molecules with a radius that is too large will have little chance of finding access to the central Ag^+ ion. Therefore, a crystal nucleus grows very slowly due to lower concentration species, and

nanoscale particles can be obtained. On the other hand, the steric effect of PVP disperses the crystal particles and reduces agglomeration.

In the present paper, a series of electrochemical investigations have been carried out on silver oxide electrodes involving nanophase Ag_2O particles. The charge–discharge behaviour of silver oxide electrodes containing different ratios of active nanophase Ag_2O particles under three different rates of discharge is demonstrated, along with the predominant electrochemical performance of a novel silver oxide electrode in comparison with a conventional electrode.

2. Experimental details

The electrochemical test setup was a three-electrode system (working, reference and auxiliary electrodes, as indicated below). 50 mg Ag_2O active species was blended with 10 mg graphite powder, ground well in an agate mortar, then a drop of 15 wt% PTFE was added as adhesive to form a tablet. This was then pressed into a slice with an area of 1 cm^2 in a cell mould. The slice was tightly contacted with a platinum sheet used as the working electrode collector. A long clean platinum rod was adopted as auxiliary electrode. The Hg/HgO reference electrode was connected to the working electrode chamber through a salt bridge with Luggin tips at both ends. The test system employed 9 mol dm^{-3} KOH as electrolyte solution.

The charge–discharge tests of this electrochemical system were conducted using an ABTS station (Arbin Co.). Before measuring, the process of formation of AgO was carried out, that is, Ag_2O was first oxidized up to a potential of 0.65 V (vs. Hg/HgO) at a low rate of $C/15$ current flow, and then this potential level was maintained for 2 h. The electrochemical cell containing the pretreated electrode was joined to the ABTS station and a charge–discharge measurement was started. There were three different discharge currents employed ($1C$, $C/3$ and $C/10$), and the corresponding cut-off voltage was −0.1, 0 and 0 V, respectively. The charge current was selected as $C/10$ and the charge cut-off voltage was 0.65 V. All experimental procedures were monitored and controlled by a computer program. The ambient temperature was about 25–26 °C.

3. Results

Six kinds of silver oxide electrodes with different proportions of nanophase Ag_2O species, which included pure electrodes with conventional, or nanophase Ag_2O, respectively, as active material, and mixed electrodes with various ratios of conventional and nanophase Ag_2O mixture were investigated. These chosen electrodes are very representative and reflect the role of active nanophase Ag_2O material on silver oxide electrodes.

Figures 1–3 show potential vs. discharge time for the various tested electrodes at currents corresponding to the $1C$, $C/3$ and $C/10$ rates, respectively. It can be seen from the plots that the rate of discharge has a distinct effect on the length and height of the potential plateaux. Under the same discharge condition, the relative amount of nanophase Ag_2O in the active material chiefly determines the length of the plateau.

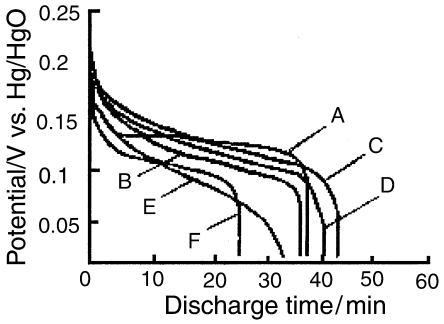

Fig. 1. Dependence of potential and discharge time of silver oxide electrode for different content of nanophase Ag_2O species under $1C$ discharge condition. (A) 30 wt % nanophase; (B) 15 wt % nanophase; (C) no nanophase (100% conventional Ag_2O); (D) 5 wt % nanophase; (E) 70 wt % nanophase; (F) 100 wt % nanophase material.

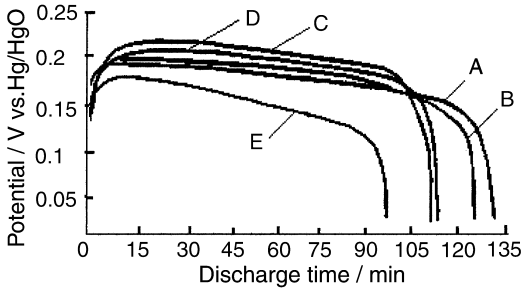

Fig. 2. Dependence of potential and discharge time of silver oxide electrode for different content of nanophase Ag_2O species under $C/3$ discharge condition. (A) 30 wt % nanophase; (B) 15 wt % nanophase; (C) no nanophase (100% conventional Ag_2O); (D) 51 wt % nanophase; (E) 70 wt % nanophase material.

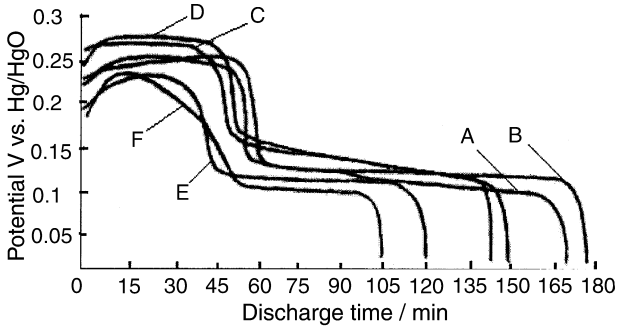

Fig. 3. Dependence of potential and discharge time of silver oxide electrode for different content of nanophase Ag_2O species under $C/10$ discharge condition. (A) 30 wt % nanophase; (B) 15 wt % nanophase; (C) no nanophase (100% conventional Ag_2O); (D) 5 wt % nanophase; (E) 70 wt % nanophase; (F) 100% nanophase material.

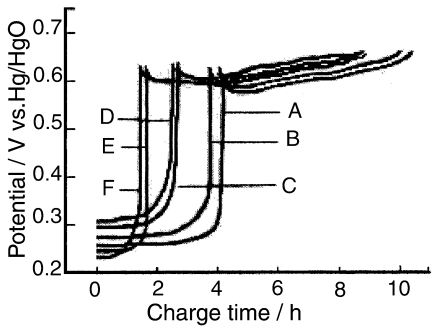

Fig. 4. Dependence of potential and charge time of silver oxide electrode for different content of nanophase Ag_2O species under $C/10$ charge condition. (A) 30 wt % nanophase; (B) 15 wt % nanophase; (C) no nanophase (100% conventional Ag_2O); (D) 5 wt % nanophase; (E) 70 wt % nanophase; (F) 100% nanophase material.

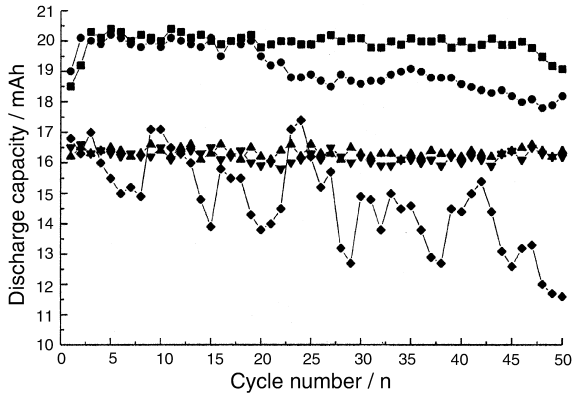

Fig. 5. Periodic discharge curves of silver oxide electrode for different content of nanophase Ag_2O species under $1C$ discharge condition. (A, ■) 30 wt % nanophase; (B, ●) 15 wt % nanophase; (C, ▲) no nanophase (100% conventional Ag_2O); (D, ▼) 5 wt % nanophase; (E, ◆) 70 wt % nanophase; (F, +) 100% nanophase material.

Figure 4 illustrates the dependence of potential of the tested electrode on the charge time at the $C/10$ current rate. There are two potential plateaux on the charge potential curves, which correspond to the two plateaux appearing on the discharge potential curves at the same $C/10$ current rate. However, in general, the charge–discharge plots indicate active nanophase Ag_2O species have more remarkable effects on discharge than charge.

The cyclic discharge capacity of various electrodes at three discharge rates is plotted in Figures 5–7. Under a discharge current condition of $1C$, the active material was stripped from the electrode (some black sediment could be seen in the electrolyte after discharge) due to the polarization caused by high current, which results in the capacity decline shown in Figure 5. In spite of this capacity loss, increasing utilization of active material by virtue of nanophase Ag_2O can be seen clearly from curves A and B. Under $C/3$ or $C/10$ discharge current conditions, the stable discharge capacity of various electrodes containing different proportions of nanophase particles has distinct differences over 50 charge–discharge cycles.

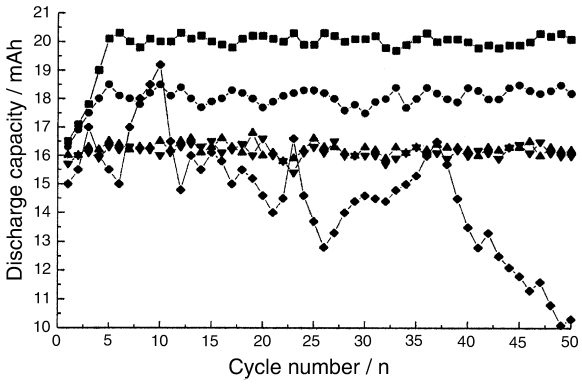

Fig. 6. Periodic discharge curves of silver oxide electrode for different content of nanophase Ag_2O species under $C/3$ discharge condition. (A, ■) 30 wt % nanophase; (B, ●) 15 wt % nanophase; (C, ▲) no nanophase (100% conventional Ag_2O); (D, ▼) 5 wt % nanophase; (E, ◆) 70 wt % nanophase material.

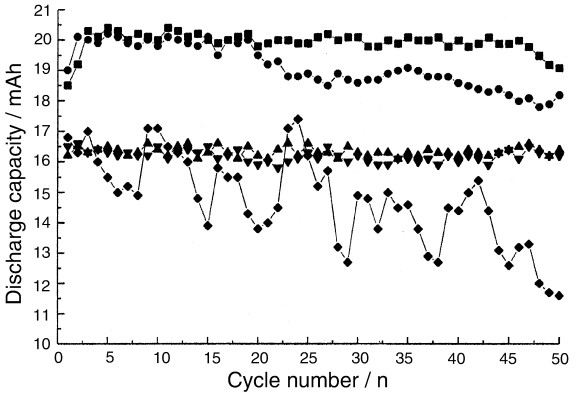

Fig. 7. Periodic discharge curves of silver oxide electrode for different content of nanophase Ag_2O species under $C/10$ discharge condition. (A, ■) 30 wt % nanophase; (B, ●) 15 wt % nanophase; (C, ▲) no nanophase (100% conventional Ag_2O); (D, ▼) 5 wt % nanophase; (E, ◆) 70 wt % nanophase material.

4. Discussion

The predominant form of active material in charged electrodes is AgO. There also exists a small quantity of Ag_2O particles because of incomplete oxidation [14]. Therefore, two potential plateaux (Figure 3) are seen on a perfect discharge curve corresponding, respectively, to Reactions 1 and 2.

$$2\,AgO + H_2O + 2\,e^- \rightarrow Ag_2O + 2\,OH^- \quad (1)$$

$$Ag_2O + H_2O + 2\,e^- \rightarrow 2Ag + 2\,OH^- \quad (2)$$

However, only one plateau appears on a high-rate discharge curve [15, 16] (Figures 1 and 2). The potential of the single plateau is, in fact, a mixed potential due to the simultaneous occurrence of Reactions 1 and 2. The emergence of a mixed potential is based on the following. When Reaction 1 occurs, the higher resistivity Ag_2O is formed and gradually covers the surface of the silver oxide electrode. The reaction resistance increases as the

charge-transfer is hindered which leads to the potential falling rapidly. The lower potential reaches a critical level and initiates Reaction 2. The product of Reaction 2, metallic Ag, having a favourable conduction, greatly improves the surface charge transfer, which makes Reaction 2 proceed more easily than Reaction 1. Obviously, the two reactions proceed almost at the same time, and Reactions 1 and 2 can be expressed as one single reaction, Reaction 3:

$$AgO + H_2O + 2e^- \rightarrow Ag + 2OH^- \quad (3)$$

The mixed potential plateau becomes much lower as the discharge rate increases, and is even below the equilibrium potential value for Reaction 2 (Figures 1 and 2). From another point of view, the total discharge capacity of one plateau (Figure 6) is equivalent to that of two plateaux (Figure 7), which also accounts for the mixed potential including either one electron in two steps as Reactions 1 and 2, or two electrons in one step as Reaction 3.

Despite the existence of a single plateau on the plot for discharge conditions of 1C and $C/3$, the difference in potential plateaux under the two discharge conditions is only 50 mV on average. It is easy to see that polarization under 1C discharge becomes severe and the initial, instantaneous potential falls very quickly as reduction continues. But the discharge plateau is higher when the electrode was discharged in $C/3$ rate. One advantage from the rising potential is that the specific energy of the silver oxide cell under the $C/3$ discharge condition is 10–15 Wh kg^{-1} higher than that under the 1C condition. The amount of electric energy output for two plateaux under the low rate ($C/10$) discharge condition is approximately equal to that of one plateau under the mid-rate ($C/3$) discharge condition. The ratio of energy output for the shorter, higher plateau compared to the long lower discharge plateau under the $C/10$ condition (Figure 3) is close to 1. It appears that the output energy of the higher plateau chiefly lies in its higher potential, and that of the lower one, mainly in its higher capacity.

As can be seen from Figures 1–3, the effect that the amount of nanophase Ag_2O species has on the electrode potential is also remarkable. If the amount of active nanophase Ag_2O species is too high (e.g., electrode E or F), the electrode potential falls quickly and does not maintain a long stable discharge. If the quantity of nanophase particles is less (e.g., electrode D), the potential curve is similar to that of electrode C (which is a conventional one), and the performance of the electrode is not obviously improved. When the nanophase Ag_2O species reaches 15–30 wt % of the active amount, the discharge curves are lengthened, which indicates augmentation of a single discharge capacity. The different results for various electrodes on the discharge potential make it clear that a certain proportion of active nanophase material optimizes the electrode and lengthens the discharge potential levels.

The plot of charge potential against time in Figure 4 also reflects the active role of nanophase Ag_2O species. A lengthening of the first charge potential plateau of electrodes A and B indicates the electrode reaction to be Reaction 4:

$$2Ag + 2OH^- \rightarrow Ag_2O + H_2O + 2e^- \quad (4)$$

Furthermore, a lower potential of the second plateau of A and B shows that the resistance of electrode Reaction 5 is smaller than any other, which results in a rise in charge efficiency, according to Reaction 5:

$$Ag_2O + 2OH^- \rightarrow 2AgO + H_2O + 2e^- \quad (5)$$

Others [17, 18] have demonstrated that the initial discharge or charge capacity is much more dependent on the effective area of the surface than on the amount of active material in the electrode. Consumption of the active material occurs only within a thin surface layer of the electrode. Therefore, the effective surface area of various tested electrodes can be compared based upon their first charged plateau or the second discharged plateau on the plot to make an evaluation of the utilization of the active material in the electrode. By this means, it is evident from the plots shown in Figures 3 and 4, that the effective surface area of electrodes A and B is relatively larger. Therefore, the active material utilization, as well as discharge capacity, is correspondingly higher than for other electrodes.

Under 1C discharge condition, the cycle life of a cell is visibly shortened because the active material strips off the electrode (Figure 5). Generally this strip-off has two explanations: dissolution of active material in the electrolyte solution and deformation of the electrode. Silver oxides such as AgO or Ag_2O have a low solubility in alkaline (e.g., KOH or NaOH) solution [19], and a heavy capacity loss does not occur. Electrode deformation is based on a variety of factors [20]. One main factor for deformation is crystal lattice distortion of active material during charge–discharge. The specific volume of charged product AgO ($d = 7.44$ g cm^{-1}) compared to discharged metallic Ag ($d = 10.9$ g cm^{-1}) is very different. When the polarizing current density is too high, an excess, or absence of, crystal oxygen atoms inevitably results, which causes heteroplasia and distortion of the crystal lattice. At a certain amount of distortion, crystal rupture occurs and, ultimately, active material strips off the electrode.

The capacity loss of active material under 1C discharge conditions is moderate from the 14th cycle, as can be seen on electrodes A and B in Figure 5. This implies that a certain quantity of active nanophase species can promote both mass and charge transfer to some extent, and raise the utilization of active material [21].

A certain proportion of active nanophase Ag_2O particles effectively fills in the voids created by conventional macro-particles. On the one hand, some inactive voids may turn into active sites and increase reaction

locations, thus optimizing the mass transfer. On the other hand, the contact among active particles become compact and make charge transfer easier. Therefore, active nanoparticles which raise the utilization of active material, optimize mass and charge-transfer and minimize electrochemical polarization.

It is noticeable, whatever the discharge conditions, that mixed electrode A demonstrates optimal electrochemical performance, and under $C/3$ or $C/10$ discharge conditions, the coulombic efficiency maintains $\sim$100% for 50 cycles of periodic charge–discharge. These favourable results are evidence that an optimal active material made up of nanophase Ag_2O species and conventional Ag_2O particles in appropriate proportions (between 1:9 and 3.5:6.5) can be used to manufacture a novel silver oxide electrode.

5. Conclusions

Some basic conclusions can be drawn as follows:

(i) Nanophase Ag_2O species has distinctive effects on electrochemical performance of various silver oxide electrodes, as follows:
   (a) If the electrode consists singly of nanophase Ag_2O as active material (e.g., F), it is unable to complete effective charge–discharge cycles.
   (b) If the proportion of nanophase Ag_2O in a mixed electrode is too high, $>$50% of the amount (e.g., E), the electrode behaviour is unstable.
   (c) If the proportion is too low, $<$5% of the amount (e.g., D), the electrochemical performance has no visible improvement compared with the conventional electrode C.
   (d) When nanophase Ag_2O is between 10 and 35% of the active amount (e.g., A and B), the periodic charge–discharge performance of the tested electrode is improved.

(ii) Compared with the conventional electrode C, the optimum mixed electrode can add an extra discharge capacity of 20–30%.

(iii) Improvement of electrochemical performance of the mixed silver oxide electrode increases active material utilization which is a result of optimum mass and charge-transfer.

References

1. C.P. Wales, *J. Electrochem. Soc.* **108** (1961) 395.
2. C.P. Wales and J. Burbant, *J. Electrochem. Soc.* **111** (1964) 1002.
3. C.K. Dyer and T.P. Hoar, *Electrochim. Acta* **20** (1975) 161.
4. V. Lazarescu, O. Radovici and M. Vass, *Electrochim. Acta* **30** (1985) 1407.
5. G.S. Popkirov, M. Burmeister and R.N. Schimdler, *J. Electroanal. Chem.* **380** (1995) 249.
6. S.L. Chen, B.L. Wu and C.S. Cha, *J. Electroanal. Chem.* **416** (1996) 53.
7. W.S. Graff and H.H. Stadelmaier, *J. Electrochem. Soc.* **105** (1958) 446.
8. J. Ambrose and R.G. Barradas, *Electrochim. Acta* **19** (1974) 781.
9. J.M.M. Droog and T. Huisman, *J. Electroanal. Chem.* **115** (1980) 211.
10. M. Lopez Teijelo, J.R. Vilche and A.J. Arvia, *J. Electroanal. Chem.* **162** (1984) 207.
11. N.A. Kotov, I. Dekany and J.H. Fendller, *J. Phys. Chem.* **99** (1995) 13065.
12. Q.W. Li, J. Li, X. Xia and Y.L. Chao, *Chinese J. Chem.* **57** (1999) 491.
13. H.T. Liu and X. Xia, *Chinese J. Chem.* **58** (2000) 992.
14. C.P. Wales and J. Burbant, *J. Electrochem. Soc.* **106** (1959) 885.
15. A. Fleischer and J.J. Lander (Eds), 'Zinc–Silver Oxide Batteries' (J. Wiley & Sons, New York, 1971).
16. K. Takeda and T. Hattori, *J. Electrochem. Soc.* **146** (1999) 3190.
17. T.P. Dirkse, *J. Electrochem. Soc.* **109** (1962) 173.
18. C.P. Wales and J. Burban, *J. Electrochem. Soc.* **112** (1965) 13.
19. T.P. Dirkse and B. Wiers, *J. Electrochem. Soc.* **106** (1959) 284.
20. R.E.F. Einerhand, W. Visscher, J.J.M. de Goeij and E. Barendrecht, *J. Electrochem. Soc.* **138** (1991) 1.
21. X. Xia and C.L. Meng, *Chin. J. Appl. Chem.* **15** (1998) 13.